Malomed, B. A., Wagenknecht, T., Champneys, A. R., & Pearce, M. J. (2005). Accumulation of embedded solitons in systems with quadratic nonlinearity.

Accumulation of embedded solitons in systems with quadratic nonlinearity

B. A. Malomed*

Department of Interdisciplinary Studies, Faculty of Engineering,

Tel Aviv University, Tel Aviv 69978, Israel

T. Wagenknecht† and A. R. Champneys‡

Department of Engineering Mathematics,

University of Bristol, Bristol, BS8 1TR, UK

M. J. Pearce§

Department of Mathematical Sciences,

Loughborough University, Loughborough, LE11 3TU, UK

(ΩDated: April 13, 2005)

Abstract

Previous numerical studies have revealed the existence of embedded solitons (ESs) in a class of multi-wave systems with quadratic nonlinearity, families of which seem to emerge from a critical point in the parameter space, where the zero solution has a fourfold zero eigenvalue. In this paper, the existence of such solutions is studied in a three-wave model. An appropriate rescaling casts the system in a normal form, which is universal for models supporting ESs through quadratic nonlinearities. The normal-form system contains a single irreducible parameter ε, and is tantamount to the basic model of type-I second-harmonic generation. An analytical approximation of WKB type yields an asymptotic formula for the distribution of discrete values of ε at which the ESs exist. Comparison with numerical results shows that the asymptotic formula yields an exact value of the scaling index, $-6/5$, and a fairly good approximation for the numerical factor in front of the scaling term.

PACS numbers: 42.81.Dp, 42.65.Tg, 02.30.Mv

*Electronic address: malomed@eng.tau.ac.il

†Electronic address: t.wagenknecht@bristol.ac.uk

‡Electronic address: a.r.champneys@bristol.ac.uk

§Electronic address: m.j.pearce@lboro.ac.uk

Soliton solutions in nonlinear models are parameterized by their intrinsic frequency. An elementary principle determines intervals of values of the frequency where ordinary solitons may be found: these must lie in gaps (semi-infinite or finite ones) in which the linearized version of the corresponding model has no solutions for radiation waves. A usual argument supporting this principle is that if one tries to construct a soliton with the frequency falling within a band occupied by the radiation-wave solutions, the soliton would start to decay by emitting linear waves whose frequency is exactly equal to the soliton's intrinsic frequency. Nevertheless, it has been demonstrated that exceptions are possible in practically important models (notably, in a system of three waves coupled by quadratic nonlinearity, with an extra linear coupling between two fundamental-frequency waves induced by a Bragg grating, in an underlying model of the spatial evolution of optical fields in a planar waveguide). These exceptional solitons, which are *embedded* in the radiation spectrum, exist as a series of isolated solutions at discrete values of the frequency inside the radiation bands. An issue of considerable interest is the evolution of these solutions following variation of governing parameters of the model: in that sense, the embedded solitons form continuous families. Previously, it was found in an empirical form (from direct numerical results) that a presumably infinite series of embedded soliton solutions emanates from a single point in the parameter plane of the above-mentioned three-wave system. The nature of this phenomenon was not understood.

In this work, we resolve these issues, by developing an asymptotic analysis and verifying the predictions against numerical results. As a result, we derive a universal asymptotic approximation (*normal form*) for models with quadratic nonlinearity that support embedded solitons. The normal form amounts to a system of two second-order equations, which is well known as a basic model for ordinary solitons in second-harmonic-generating systems. There was a rather common belief that all soliton solutions had been found in this much-studied system. Nevertheless, in this work we are able to predict the existence of an infinite series of previously unknown embedded solitons in the model. This is done in an analytical form, by realizing that the embedded solitons feature a broad inner zone, the solution in which must be matched to exponentially decaying ones in outer zones. Further, a method (Bohr-Sommerfeld quantization rule) borrowed from quantum mechanics is applied to the solution in the inner zone. The most essential part of the eventual analytical result is an asymptotic distribution law for values of the single control parameter of the normal-form system at which the embedded solitons exist. Comparison with numerical results clearly shows that the analysis has produced an *exact* value of the respective scaling index.

I. INTRODUCTION

This article deals with spatial solitary waves (or solitons in short, without implying integrability of the underlying model) in a model of a planar waveguide with a quadratic

(χ^2) nonlinearity, where two fundamental-frequency (FF) waves, $u_1$and u_2, are linearly coupled by the Bragg reflection from a grating of ridges or grooves on the surface of the waveguide. The waves are coupled into the waveguide so that their amplitudes evolve along the direction z, which is aligned with the Bragg grating, the Poynting vectors of the two FF waves having angles $\pm\alpha$ with the z axis (where the angle α is small). The $\chi^{(2)}$-induced nonlinear coupling between the FF waves generates a second-harmonic (SH) wave, u_3. The corresponding dimensionless model, derived in Ref. [1], amounts to a system of normalized equations,

$$\begin{aligned} i(u_1)_z + i(u_1)_x + u_2 + u_3 u_2^* &= 0, \\ i(u_2)_z - i(u_2)_x + u_1 + u_3 u_1^* &= 0, \\ 2i(u_3)_z - qu_3 + D(u_3)_{xx} + u_1 u_2 &= 0, \end{aligned} \tag{1}$$

where x is the transverse coordinate, the opposite signs in front of the walk-off terms $(u_{1,2})_x$ correspond to the above-mentioned opposite angles $\pm\alpha$ (α itself does now appear in the equations as it can be removed by a rescaling), the asterisk stands for complex conjugation, and real coefficients D and q account for the intrinsic diffraction and wave-number mismatch of the SH wave (the intrinsic diffraction of the FF waves is neglected, as the artificial diffraction, induced through the interplay of the Bragg-grating-induced linear coupling and opposite walk-off terms, is stronger by several orders of magnitude). Note that (1) is invariant with respect to both a shift of phase by an arbitrary real constant ϕ,

$$S : (u_1, u_2, u_3) \mapsto (\exp(i\phi)u_1, \exp(i\phi)u_2, \exp(2i\phi)u_3), \tag{2}$$

and to an arbitrary transverse shift.

Solitary waves in Eqs. (1) have been investigated in several works [1–4]. The

present work was motivated by results in the two latter references, which had produced *embedded solitons* (ESs) in the system. ESs are distinguished by the feature that their internal frequency (spatial frequency or propagation constant, in the present context) is in resonance with radiation waves, [5]. In general, one expects to find quasi-solitons with non-vanishing oscillating tails in such a case. However, at certain discrete values of the frequency, the amplitude of these tails can exactly vanish, thus giving rise to a truly localized solution with a frequency that is *embedded in* the continuous spectrum.

One may seek for stationary ES solutions of (1) in the form

$$u_{1,2}(x,z) = \exp(ikz)U_{1,2}(\xi), \qquad u_3(x,z) = \exp(2ikz)U_3(\xi) \tag{3}$$

where k denotes the wave number, and $\xi = x - cz$ is the tilted ("walking") coordinate, with c measuring the walk-off of the spatial soliton's axis relative to the propagation direction z. Substitution of the ansatz (3) into (1) leads to a system of ordinary differential equations for the complex amplitudes U_i,

$$\begin{aligned} -kU_1 + i(1-c)U_1' + U_2 + U_3U_2^* &= 0, \\ -kU_2 - i(1+c)U_2' + U_1 + U_3U_1^* &= 0, \\ -(4k+q)U_3 + DU_3'' - 2icU_3' + U_1U_2 &= 0, \end{aligned} \tag{4}$$

with the prime standing for $d/d\xi$.

The analysis in this paper will concentrate on standing solitons with $c = 0$, in which case we can set $D = 1$ with no loss of generality. Furthermore, Eqs. (4) with $c = 0$ allow for symmetry reductions to four-dimensional invariant subspaces, the phase-shift-invariance (2) accounting for the existence of a one-parameter family of such invariant spaces. Localized solutions can be studied in any member of this family. A convenient

FIG. 1: Enter Figure 1 here.

reduction is achieved by setting $U_1 = -U_2 \equiv V \equiv V_1 + iV_2$ (V_1 and V_2 are real), $U_3 = U_3^* \equiv W$ (i.e., W is real), which reduces Eqs. (4) to a system

$$\begin{aligned} -kV + iV' - VW - V^* &= 0, \\ -(4k+q)W + W'' - |V|^2 &= 0. \end{aligned} \tag{5}$$

A linear analysis reveals the region in parameter space where ESs may be found. Indeed, in order for ESs to exist, the zero solution of Eqs. (5), $V = W = 0$, has to be a *saddle-center*, i.e., the spectrum of the linearized system has to contain a pair of real eigenvalues, such that solutions exponentially localized in one direction exist, and a pair of purely imaginary eigenvalues, that account, in the general case, for non vanishing tails in another direction (if all the eigenvalues are real, the system gives rise to ordinary gap solitons instead of ESs, [5]). For Eqs. (5), it is straightforward to find that the zero solution is a saddle-center in the region of the parameter space determined by the inequalities

$$k^2 < 1, \ 4k + q < 0, \tag{6}$$

see also Fig. 1.

An important property of Eqs. (5) is *reversibility*. This means its invariance under the transformation (involution)

$$R_1 : (V, W, W') \mapsto (V^*, W, -W'), \quad \xi \mapsto -\xi. \tag{7}$$

An ES of Eqs. (1) must be a solution of Eqs. (5) homoclinic to the saddle-center 0. For such a solution to exist, the one-dimensional stable and unstable manifolds of the equilibrium have to agree along the solution, and in general this situation is of codimension

three in $\mathbb{R}^4$. However, in an R_1-reversible system obeying the invariance (7), the stable and unstable manifolds of 0 are R_1-images of one another. Thus, a homoclinic orbit to 0 exists if the unstable manifold of 0 intersects the two-dimensional fixed subspace of the full four-dimensional phase space of Eqs. (5), $\mathrm{Fix}(R_1) = \{V_2 = W' = 0\}$. This is a codimension-one situation and consequently, ESs should exist for parameter values on curves in the two-dimensional parameter plane of the system (5). Homoclinic orbits that intersect the fixed space of the involution (7) are themselves invariant under its action, therefore they are called symmetric.

Remark 1 *In addition, system (5) is reversible with respect to a second involution,*

$$R_2 : (V, W, W') \mapsto (-V^*, W, -W'), \quad \xi \mapsto -\xi. \tag{8}$$

According to the behavior of the first FF wave, V_1, we will call ESs that are symmetric with respect to R_1 even and those symmetric with respect to R_2 odd. (Note that the SH (W) component of both R_1- and R_2-symmetric homoclinic solutions is automatically even.)

Remark 2 *This paper deals with fundamental ESs of (1), i.e., one-pulse (single-humped) homoclinic solutions of Eqs. (4) or (5). It is well known that N-pulse homoclinic orbits can emerge in bifurcations of homoclinic orbits to saddle-center equilibria . In particular, it can be shown that families of 2-pulse homoclinic orbits (bound-state solitons) must accumulate on a family of ESs [6, 7].*

It is straightforward to numerically construct both even and odd ESs, using a variant of a numerical shooting method proposed in [8], which searches for intersections of the

FIG. 2: Enter Figure 2 here.

unstable manifold of 0 with the corresponding fixed spaces $\mathrm{Fix}(R_{1,2})$. Afterwards, branches of these solutions can been continued using the software package AUTO [9]. The corresponding results have already been reported in Refs. [3, 4].

Figure 2 gives a concise overview of the computed branches of ESs for Eqs. (5). In this paper, we are interested in the situation close to the line $4k + q = 0$. If this curve is crossed (with $|k| < 1$), the 0 equilibrium changes its type from a saddle-center into a saddle. It has been shown in Ref. [10] that there is a possibility for curves of ES solutions to approach this curve transversally. In that case, if the curve is crossed, the soliton is not destroyed but rather changes its type from embedded to an ordinary gap soliton. As can be seen in Figure 2, this scenario *does not* occur for system (5). Instead, one finds that all the curves of the ES solutions approach the point $k = 1, q = -4$, becoming asymptotically tangent to the line $4k + q = 0$. For these parameter values 0 is a degenerate codimension-two point, whose linearization produces a fourfold zero eigenvalue. Our aim in this paper is to understand how families of ESs accumulate at (emanate from) this point.

In order to understand this accumulation we will perform an asymptotic analysis of ES solutions. The analysis, however, will not be performed directly for Eqs. (5). Instead, we perform a rescaling of the original problem and derive a suitable normal form in Section II. Afterwards, in Section III, an analytical WKB approximation yields asymptotic estimates for parameter values at which ES solutions are predicted to exist. The theory is verified by numerical results.

FIG. 3: Enter Figure 3 here.

II. THE TWO-WAVE SYSTEM AS A NORMAL FORM

The analysis of Eqs. (5) is facilitated by a rescaling of the equations, suggested by the numerically computed solutions. First, we display examples of such solutions. Fig. 3 shows the FF and SH components of ES solutions, which have been computed along the line $k = 0$. It can be seen that the FF component features internal oscillations, with the number of oscillations increasing as the line $4k + q = 0$ is approached. At the same time, the SH component keeps a single-humped shape, with an increasing amplitude.

It is interesting to interpret these numerical observations geometrically. Note that geometric arguments have been successfully used in Ref. [10] to understand the transition from ESs to ordinary gap solitons (however, that work does not explain why this transition is absent in the system (5)).

Observe first that in the region $k^2 < 1$ and $4k + q < 0$, where the ESs exist, the 0-equilibrium has a two-dimensional center manifold $\mathcal{W}^c$, which is filled with periodic orbits. In fact, from Eqs. (5) it can be seen that the flow in $\mathcal{W}^c$ obeys the linear equation

$$W'' = (4k + q)W,$$

which gives rise to periodic solutions with arbitrarily large amplitude. This explains the (unusual) behavior of the ES solutions, shown in Figure 3. More precisely, for different branches of the ESs in Eqs. (5), the SH component W grows indefinitely when the line $4k + q = 0$ is approached. At the same time, the FF component, which corres-

ponds to the hyperbolic direction of the 0-equilibrium, shrinks and develops more and more internal oscillations. Thus, in the (V_1, V_2, W, W') phase space, the corresponding homoclinic orbit follows a periodic orbit in $\mathcal{W}^c$, thereby oscillating around $\mathcal{W}^c$. Both the size of the periodic orbit that is followed and the number of oscillations around $\mathcal{W}^c$ increase as $4k + q = 0$ is approached.

Although these geometric considerations give insight into the behavior of Eqs. (5), they do not explain the most remarkable feature, viz., the accumulation of branches of the ESs at $k = 1$, $q = -4$. In fact, since the 0-equilibrium has a four-dimensional center manifold for these parameter values, even the local behavior near this equilibrium is completely unknown *a priori*. We therefore address the existence of ES solutions via an asymptotic analysis of a normal-form system derived below.

To this end, we again consider Eqs. (4) with $c = 0$, but this time reduced to the invariant subspace $U_1 = U_2^* \equiv V$, $U_3 = U_3^* = W$. Being interested in the behavior near $k = 1$ and $q = -4$, we define $\alpha \equiv k-1$, $\beta \equiv 4k+q$. Recall that due to the invariance of (4) with respect to S, the results will not depend on the choice of a particular invariant subspace.

The equations for V and W then read

$$\begin{aligned} -iV' - \alpha V - (V - V^*) + VW &= 0, \\ W'' - \beta W + |V|^2 &= 0. \end{aligned} \tag{9}$$

The scaling $\beta = \alpha\varepsilon$, $\xi = (-\alpha)^{-1/2}x$, $V_1 = (-\alpha)v_1$, $V_2 = (-\alpha)^{3/2}v_2$, and $W = (-\alpha)w$

transforms this system into

$$\begin{aligned} v_1' &= (2+\alpha)v_2 + \alpha v_2 w, \\ v_2' &= v_1 + v_1 w, \\ w'' &= -\varepsilon w - v_1^2 + \alpha v_2^2, \end{aligned} \tag{10}$$

where the prime now stands for d/dx. We are interested in solutions at $\alpha \ll 1$, for which $|v_2| \ll |v_1|$. In this case, Eqs. (10) can be further simplified to

$$\begin{aligned} v_1' &= 2v_2, \\ v_2' &= v_1 + v_1 w, \\ w'' &= -\varepsilon w - v_1^2, \end{aligned} \tag{11}$$

or, setting $v \equiv v_1$, to a system of two second-order equations,

$$\begin{aligned} v'' &= 2v + 2vw, \\ w'' &= -\varepsilon w - v^2. \end{aligned} \tag{12}$$

System (12) describes stationary solutions in optical models with the χ^2 nonlinearity of the so-called type I, which means that the system contains only two wave fields, rather than three. It has been studied in detail by a number of authors, see the reviews [11, 12]. The case we are interested in, with $\varepsilon > 0$, is generally classified as the "bright-dark" case, where the latter precisely means that it may have generic solutions localized in one direction only. We view Eqs. (12) as a *normal form* for a class of models supporting embedded solitons through quadratic nonlinearity.

Remark 3 *Note that Eqs. (12) can also be interpreted in the context normal form theory, as, for example, introduced in [13]. Choosing the coefficient in front of the linear term in the equation for v to be another parameter, say μ, instead of the constant*

value 2*, Eqs. (12) describe a normal form for equilibria with fourfold eigenvalue zero in the class of reversible systems. It is interesting to note that the general normal form contains an additional quadratic term* w^2 *in the equation for* w*. The fact that this term is missing in (12) shows the special (degenerate) character of the equations. (Note that this also implies a purely linear flow* $w'' = -\varepsilon w$ *in the centre manifold of the system.) Consequently, former studies of normal forms near equilibria with fourfold eigenvalue zero in [14, 15] do not discuss the accumulation of ESs observed in Eqs. (12).*

We shall now proceed with an asymptotic analysis to find a *new class* of solutions to the much-studied equations (12); to the best of our knowledge, the numerous previous studies of the system did not discuss the solutions that we report on below. Note that the solutions have an unfeasibly large w component and were probably missed because of that. Furthermore, as stationary solutions to the full type-I $\chi^{(2)}$ model, these solitons are likely to be unstable, but they are, nevertheless, of importance for the understanding of the normal forms and intrinsic structure of the $\chi^{(2)}$ models.

III. ANALYSIS OF EMBEDDED SOLITONS BY MEANS OF THE WKB APPROXIMATION

We are interested in the existence and shape of ES solutions of Eqs. (12) in the limit $\varepsilon \to +0$. After applying the transformation to map solutions of Eqs. (9) into those of Eqs. (12), we find that in this limit the w-component becomes large and wide, while the v-component oscillates in an effective potential induced by $w(x)$ within this inner core. Note that we focus on detecting even ES solutions of (12), which are the

fundamental ones.

A. Inner zone analysis

We first consider the core of the ES solution, that is, values of x, for which w does not decay to 0. Here we we shall look for solutions of Eqs. (12) via the ansatz

$$\begin{aligned} v(x) &= v_0(\delta x)\sin(\phi(x)), \\ w(x) &= -w_0(\sqrt{\delta}x) + w_2(\delta x)\cos(2\phi(x)). \end{aligned} \tag{13}$$

Here it is assumed that $\delta \ll 1$, such that v_0, w_0 and w_2 are slowly varying functions.

Substitution of the ansatz (13) into Eqs. (12) and equating coefficients in front of $\sin\phi$ and $\cos\phi$ leads, in the lowest-order approximation, to the following equations:

$$\phi'^2 = 2\left(w_0 - 1\right), \tag{14}$$

$$\frac{d}{dx}\left(v_0^2\phi'\right) = 0, \quad \Longrightarrow v_0^2 = \frac{2C}{\sqrt{w_0 - 1}}, \tag{15}$$

where C is an arbitrary integration constant, and the factor 2 was introduced for convenience. Observe that Eq. (15) requires $w_0 > 1$. Next, substituting Eqs. (13), and (14), (15) into the equation for w in system (12), and equating coefficients as above, yields the following results:

$$\frac{d^2 w_0}{dx^2} + \frac{\varepsilon}{\delta}w_0 - \frac{C}{\delta\sqrt{w_0 - 1}} = 0, \tag{16}$$

$$w_2 = -\frac{v_0^2}{2\left(4\phi'^2 - \varepsilon\right)} \equiv -\frac{C}{\sqrt{w_0 - 1}\cdot\left(8\left(w_0 - 1\right) - \varepsilon\right)}. \tag{17}$$

After the rescaling $\xi \equiv \sqrt{\varepsilon/\delta}x$, Eq. (16) may be represented as

$$\frac{d^2 w_0}{d\xi^2} = -\frac{dP\left(w_0\right)}{dw_0}, \tag{18}$$

i.e., as the equation of motion for a classical particle with mass $m = 1$ and the coordinate w_0, in a potential

$$P(w_0) \equiv \frac{1}{2}\left(w_0^2 - 1\right) - K\sqrt{w_0 - 1}, \quad K \equiv \frac{2C}{\varepsilon}. \tag{19}$$

In order for Eqs. (13) to describe ES solutions of Eqs. (12), which vanish at infinity, we must equate the conserved energy of the mechanical model (18) to zero, $(1/2)\left(w_0'\right)^2 + P(w_0) = 0$. This equation can be solved via the substitution

$$w_0(\xi) = 1 + \eta^4(\xi), \tag{20}$$

which yields an implicit solution,

$$\xi = \int_0^{\eta_0} \frac{4\eta^2}{\sqrt{2K - 2\eta^2 - \eta^6}}\, d\eta. \tag{21}$$

Here, η_0 is a solution of

$$2K - 2\eta^2 - \eta^6 = 0. \tag{22}$$

This implicit solution will be sufficient for the subsequent analysis.

B. The Bohr-Sommerfeld quantization of the constant C

Using the above results, we can apply the *Bohr-Sommerfeld* (BS) quantization rule (a part of the semi-classical or WKB approximation in quantum mechanics), which selects a discrete spectrum of values of ε, necessary for the existence of the ES solution. Recall that the analysis so far has been valid for the case of $w_0 > 1$. If $w_0 = 1$, then $\phi' = 0$, because of Eq. (14), and we face a turning-point problem. Moreover, $w_0(x) = 1$ leads to a divergence in Eq. (15), which has to be compensated by setting

$\sin(\phi(x)) = 0$. Obviously, there are two values of x for which $w_0(x) - 1$ vanishes. In fact, these points describe the transition from the core of the ES to its asymptotic tails, where the solution decays to 0. At one of the two points, say $x = 0$, we simply set $\phi = 0$. Then the condition that $\sin\phi$ also vanishes at the second point, $x = X$, implies that

$$\phi(X) = \int_0^X \phi'(x)dx = n\pi,\ n = 1, 2, 3, ... \tag{23}$$

Observe that n counts the number of "inner oscillations" of the v-component of the derived solution. We thus obtain

$$\begin{aligned} n\pi &= \int_0^{\sqrt{\varepsilon}X} \sqrt{\frac{2}{\varepsilon}}\ \eta^2(\xi)\ d\xi \\ &= \int_0^{\eta_0} \sqrt{\frac{2}{\varepsilon}}\ \frac{4\eta^4}{\sqrt{2K - 2\eta^2 - \eta^6}}\ d\eta. \end{aligned} \tag{24}$$

Equation (24) is tantamount to the BS rule in the semi-classical limit of quantum mechanics.

We now have to distinguish two cases. First we assume $K \ll 1$. In this case we obtain from Eq. (22) that $\eta_0 \approx \sqrt{K}$, and the BS rule yields

$$\sqrt{\frac{2}{\varepsilon}} \int_0^1 \sqrt{K} \frac{4K^2\tau^4}{\sqrt{2K - 2K\tau^2 - K^3\tau^6}}\ d\tau = n\pi. \tag{25}$$

In particular, for small ε, making use of the fact that

$$\int_0^1 \frac{\eta^4 d\eta}{\sqrt{1 - \eta^2}} = \frac{3}{16}\pi, \tag{26}$$

the BS quantization rule takes an eventual explicit form,

$$K_n^2 = \frac{4}{3}\sqrt{\varepsilon}n. \tag{27}$$

On the other hand, for large $K \gg 1$, we have $\eta_0 = 2K^{1/6}$. In a similar way, using the numerical value

$$\int_0^1 \frac{\tau^4}{\sqrt{1-\tau^6}}\, d\tau = \frac{\Gamma\left(2/3\right)\Gamma\left(5/6\right)}{4\sqrt{\pi/3}} \approx 0.373, \tag{28}$$

the BS rule leads to

$$\left(2K_n\right)^{1/3} = \frac{n\pi}{4\sqrt{2}\cdot 0.373}\sqrt{\varepsilon}. \tag{29}$$

C. The asymptotic solution in the outer zone, and quantization of ε

The above analysis has been dealing with the *inner zone* (core) of the ES solution, where w_0 took values $w_0 \geq 1$. It remains to match the results to the solution in the *outer zone* (tail), where w_0 decays to 0. To this end, we note first that the solution for the fundamental field, which takes the form of Eq. (13) in the inner zone, can be matched to an exponentially decaying solution for the same field in the outer zone, given by

$$v_{\text{outer}}(x) = A\exp\left(-\sqrt{2}|x|\right). \tag{30}$$

The actual issue is to relate the constant A in this expression to C in Eq. (15). This can be done using the known *connection formula* [16] of the WKB approximation, with the result

$$A = \sqrt{C/2}. \tag{31}$$

In the same outer zone, we can use the fact that the ES is a localized solution. This implies that the corresponding solution for the SH field is

$$w(x) \approx B\exp\left(-2\sqrt{2}|x|\right). \tag{32}$$

The amplitude B can be computed using the differential equation (12) for w and relation (31). We thus find

$$B = -A^2/8 = -C/16. \tag{33}$$

Now, we can match the outer and inner solutions for the SH field, demanding continuity of this field. According to the above results, the inner-field solution takes the value $(w)_{\text{inner}}(x = 0) = -w_0(x = 0) = -1$, see again (13), at the border between the two zones. The matching condition thus implies $C = 16$, and therefore we find

$$\varepsilon K_n = 32. \tag{34}$$

It should be noted that this matching procedure is not a rigorous one, which would demand to construct an intermediate asymptotic solution in a transient zone, whose functional form (rather than just values of the fields at the contact points) must be matched to ones in the inner and outer zones. Such a rigorous procedure would be extremely complicated in the present system, while the simpler one described above yields, eventually, rather accurate results, as shown below.

We can now use the "quantization rules" (27) and (29) to derive approximations for values ε_n at which ES solutions exist in system (12). We again start with the case $K \ll 1$. The above considerations show that

$$\varepsilon_n = \frac{32}{K_n} = \frac{16\sqrt{3}}{\sqrt{\varepsilon_n} n^{1/2}}, \tag{35}$$

and therefore,

$$K_n = \frac{32}{(16\sqrt{3})^{4/5}} \cdot n^{2/5}. \tag{36}$$

However, this implies $K_n \to \infty$ for $n \to \infty$, in contrast to $K \ll 1$. So this case is irrelevant.

In the opposite case, when K is large, the combination of Eq. (34) and the corresponding approximation (29) produces the result

$$\varepsilon_n = 3.27 \cdot n^{-6/5}. \tag{37}$$

The applicability of this result also demands n to be large enough. The condition $K \gg 1$, which was used to derive Eq. (37), now reduces to $32/\varepsilon_n \approx 9.8 \cdot n^{6/5} \gg 1$, which is *always satisfied*. So, Eq. (37) yields an asymptotic formula for values of ε_n at which Eqs. (12) support ES solutions.

D. Numerical verification

We now investigate the validity of the analytical prediction result (37) through numerical solution of Eqs. (12). Similar to the case of system (5), ES solutions can be computed by searching intersections of the unstable manifold of 0 with $\mathrm{Fix}(R)$ by dint of the shooting method. This way, the first 140 solutions have been constructed. The results are summarized in Fig. 4. In the main panel e) we plot $n^{-6/5}$ against ε, where n is identified as the number of oscillations of the v-component in the solution's inner zone, following the consideration of the soliton's structure presented above in Section III. For $n = 1, 2, 10, 20$, the computed solutions are shown in panels a) - d). Panel f) specially displays a zoom of the small square from e), which corresponds to $50 \leq n \leq 140$. For these values of n we may reasonably assume may Eq. (37) to be applicable. Again, the axes are chosen to be $n^{-6/5}$ and ε with the objective to compare the numerical and analytical results.

A linear regression analysis for the close-up in panel f) yields the following fit to

FIG. 4: Enter Figure 4 here.

the computed values,

$$\varepsilon_n = 6 \cdot 10^{-5} + 2.8247 \cdot n^{-6/5}, \tag{38}$$

which is also shown in Fig. 4(f). First of all, it corroborates the main result of the above asymptotic analysis, viz., that the *scaling index* for ε_n is $-6/5$. Further, the numerical factor in front of $n^{-6/5}$, predicted by Eq. (4), and its empirical counterpart in Eq. (38) differ by $\simeq 15\%$. This moderate discrepancy may be explained by the insufficiently accurate matching procedure, as discussed above. Finally, the very small constant term in Eq. (38) is actually caused by the contribution from the ES solutions with smaller n, to which the asymptotic analysis does not apply. In particular, limiting the numerical data to $80 \leq n \leq 140$ reduces the constant term by a factor of 6, and shows that all the data fall into a 95%–confidence interval corresponding to a strictly proportional relation between ε_n and $n^{-6/5}$, without the constant term in Eq. (38).

IV. CONCLUSIONS

In this paper, we have derived a system of two second-order equations with one free parameter, ε, as an asymptotic normal form of models with quadratic nonlinearity, close to a critical point from which branches of embedded-soliton (ES) solutions originate. At the critical point the zero solution possesses a fourfold eigenvalue zero.

The derived normal form equations are tantamount to a well-known system, which is fundamental for the usual second-harmonic-generation model of type I. Despite the fact that the system has been much studied, we were able to find a new infinite series of

ES solutions in this work. A fundamental characteristic of the series is an asymptotic distribution law for discrete values of ε at which the ES exist. Making use of the Bohr-Sommerfeld quantization rule borrowed from the semi-classical version of quantum mechanics and a simplified procedure of matching the solutions in the inner and outer zones of the soliton we were able to predict the asymptotic distribution law in a fully analytical form. The comparison with direct numerical results shows that the predicted scaling law, $\varepsilon_n = \text{const} \cdot n^{-6/5}$, may be absolutely exact (no discrepancy in the value of the scaling index, $-6/5$, was found), and the constant factor was predicted with an error $\simeq 15\%$ (due to an inaccuracy of the simplified matching procedure).

These results present fundamental (and previously unknown in any form) information about families of ES solutions in multi-wave systems with quadratic nonlinearity. Additionally, they shed new light on the above-mentioned system (12) that describes type-I second-harmonic generation.

It is worthwhile to contrast the features of the families of ESs that we have established with other infinite families of ESs found in the literature, e.g. [5, 17, 18]. In all other cases we are aware of the individual members of the family correspond to multi-humped solitary waves. In contrast, our construction produces waves that are fundamental in one component and become highly oscillatory in the second component. Effectively these are single-humped waves.

There are chiefly two mechanism that produce multi-humped waves, under a so-called Birkhoff signature condition on the sign of the nonlinear term. This condition is satisfied by the three-wave system investigated here. One theory (see remark 2 above) shows that there must be an infinite family of branches of multi-humped ESs

accumulating on each branch of single-humped ES. The other theory [18] shows that multi-humped waves must accumulate on the limit corresponding to $k = 1$ in this model. Further numerical results not presented here [4] compute representatives of both kinds of multi-humped ESs and follow their branches in the (k, q)-plane. Note that the latter kind also produces a family of curves that originate from the point $q = -4, k = 1$ in Figure 2 [4, Fig 4.3] similar to the families computed by Yang and Akylas [17] for the third-order nonlinear Schrödinger equation. The aim of this paper has been to establish why in addition, an infinite family of *single-humped* solitons should emanate from the same critical point in the three-wave model.

We have already pointed out that we do not expect these newly-established families of excited ESs to be stable for the full PDE system. This has been demonstrated in numerical studies for the 3-wave system (1) in [4]. Nevertheless, it has also been shown there that if the parameters are chosen close enough to the critical value, the even ground-state solution shown in the top panel of Figure 3 is *virtually stable*. This means that although the central cores emit radiation tails, those have an extremely small amplitude and it takes a considerable distance for the soliton solution to show instability. We would expect that the excited states would also develop very slow instabilities near to the critical point. Thus, there may be physical application of these multitude of states, for example in optical memory, as in most experimental systems the residence time is much smaller than that required to produce the instability.

Acknowledgement

B.A.M. appreciates hospitality of the Department of Engineering Mathematics at the University of Bristol under support of EPSRC grant GR/R72020/01 (BCANM). T.W. acknowledges support by EPSRC grant GR/535684/01.

---

[1] W. C. K. Mak, B. A. Malomed, and P. L. Chu. Three-wave gap solitons in waveguides with quadratic nonlinearity. *Physical Review E*, 58:6708–6722, 1998.

[2] J. Schöllmann and A. P. Mayer. Stability analysis for extended models of gap solitary waves. *Physical Review E*, (61):5830–5838, 2000.

[3] A. R. Champneys and B. A. Malomed. Embedded solitons in a three-wave system. *Phys. Rev. E*, 61:463–466, 1999.

[4] M. J. C. Pearce. *Embedded Solitons in a Three-Wave System*. PhD thesis, University of Bristol, 2003.

[5] A. R. Champneys, B. A. Malomed, J. Yang, and D. J. Kaup. Embedded solitons: solitary waves in resonance with the linear spectrum. *Physica D*, 152:340–354, 2001.

[6] A. R. Champneys and J. Härterich. Cascades of homoclinic orbits to a saddle-centre for reversible and perturbed Hamiltonian systems. *Dynamical Systems*, 15:231–252, 2000.

[7] A. Mielke, P. Holmes, and O. O'Reilly. Cascades of homoclinic orbits to, and chaos near, a Hamiltonian saddle-center. *J. Dynamics Diff. Eqns.*, 4:95–126, 1992.

[8] A. R. Champneys and A. Spence. Hunting for homoclinic orbits in reversible systems: a shooting technique. *Advances in Computational Mathematics*, 1:81–108, 1993.

[9] E. J. Doedel, A. R. Champneys, T. R. Fairgrieve, Yu. A. Kuznetsov, B. Sandstede, and X. J. Wang. AUTO97 continuation and bifurcation software for ordinary differential equations, 1997. Available by anonymous ftp from FTP.CS.CONCORDIA.CA, directory PUB/DOEDEL/AUTO.

[10] T. Wagenknecht and A. R. Champneys. When gap solitons become embedded solitons: a generic unfolding. *Physica D*, 177:50–70, 2003.

[11] C. Etrich, F. Lederer, B. A. Malomed, T. Peschel, and U. Peschel. Optical solitons in media with a quadratic nonlinearity. *Progress in Optics*, 41:483–568, 2000.

[12] A. V. Buryak, P. Di Trapani, D. V. Skryabin, and S. Trillo. Optical solitons due to quadratic nonlinearities: from basic physics to futuristic applications. *Physics Reports*, 370:63–235, 2002.

[13] C. Elphick, E. Tirapegui, M. Brachet, P. Coullet, and G. Iooss. A simple global characterisation for normal forms of singular vector fields. *Physica D*, 29:95–127, 1987.

[14] G. Iooss. A codimension-two bifurcation for reversible vector fields. *Fields Institute Communications*, 4:201–217, 1995.

[15] T. Wagenknecht. Bifurcation of a reversible Hamiltonian system from a fixed point with fourfold eigenvalue zero. *Dynamical Systems*, 17(1):29–45, 2002.

[16] C. M. Bender and S. Orszag. *Advanced Mathematical Methods for Scientists and Engineers*. McGraw-Hill, 1978.

[17] J. Yang and T. R. Akylas Continuous families of embedded solitons in the third-order nonlinear Schrödinger equation. *Studies in Applied Math.* 111:359-375, 2003.

[18] K. Kolossovski A. R. Champneys A. V. Buryak and R. Sammut Multi-pulse embedded

solitons as bound states of quasi-solitons. *Physica D* 171:153-177, 2002.

List of Captions

FIG. 1: Results of the linear analysis predicting the possible existence of embedded solitons in the case of $D = 1$. In each part of the parameter plane, the set of eigenvalues found from the equations (5) linearized around the zero solution is displayed.The large dot at $(k, q) = (1, -4)$ denotes a codimension-two point at which the linearized system has a fourfold eigenvalue zero.

FIG. 2: Branches of even (dotted curves) and odd (solid curves) ESs in system (5), as per Ref. [4]. No branch crosses the line $4k+q = 0$, but all of them approach the point $(k, q) = (1, -4)$ tangentially to this line.

FIG. 3: Examples of even (left panels) and odd (right panels) embedded-soliton solutions of Eqs. (5), computed for $k = 0$, as per Ref. [4]. Recall that V_1 and V_2 are the real and imaginary parts of the complex field V.

FIG. 4: Panels a) through d) show characteristic examples of the embedded solitons found from the numerical solution of Eqs. (12). 140 values of ε at which the embedded solitons are found are collected in the main box e), n being identified as the number of oscillations of the v-component in the soliton's inner zone. Panel f) is a close-up of a part of the main diagram for $50 < n < 140$. It also shows the straight line (38) which provides for the best fit to the data included in this panel.

Figure 1

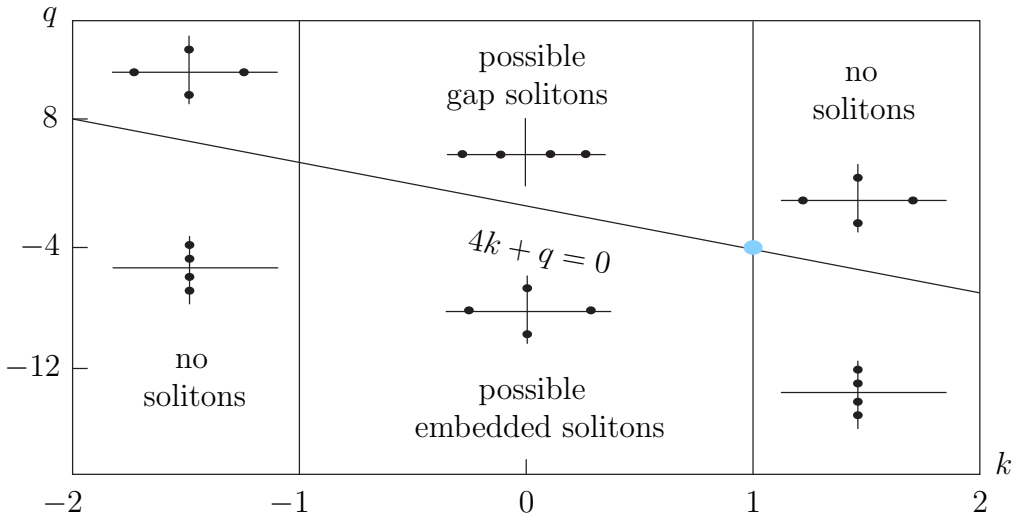
q
8
−4
−12
possible
gap solitons
no
solitons
4k + q = 0
no
solitons
possible
embedded solitons
k
−2
−1
0
1
2

Figure 2

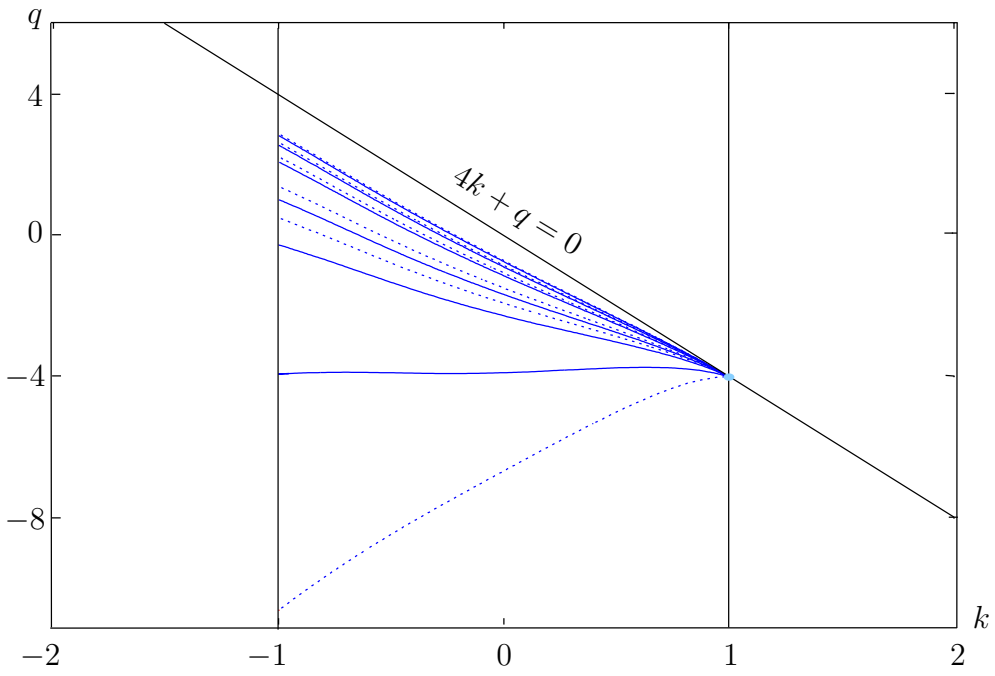

Figure 3

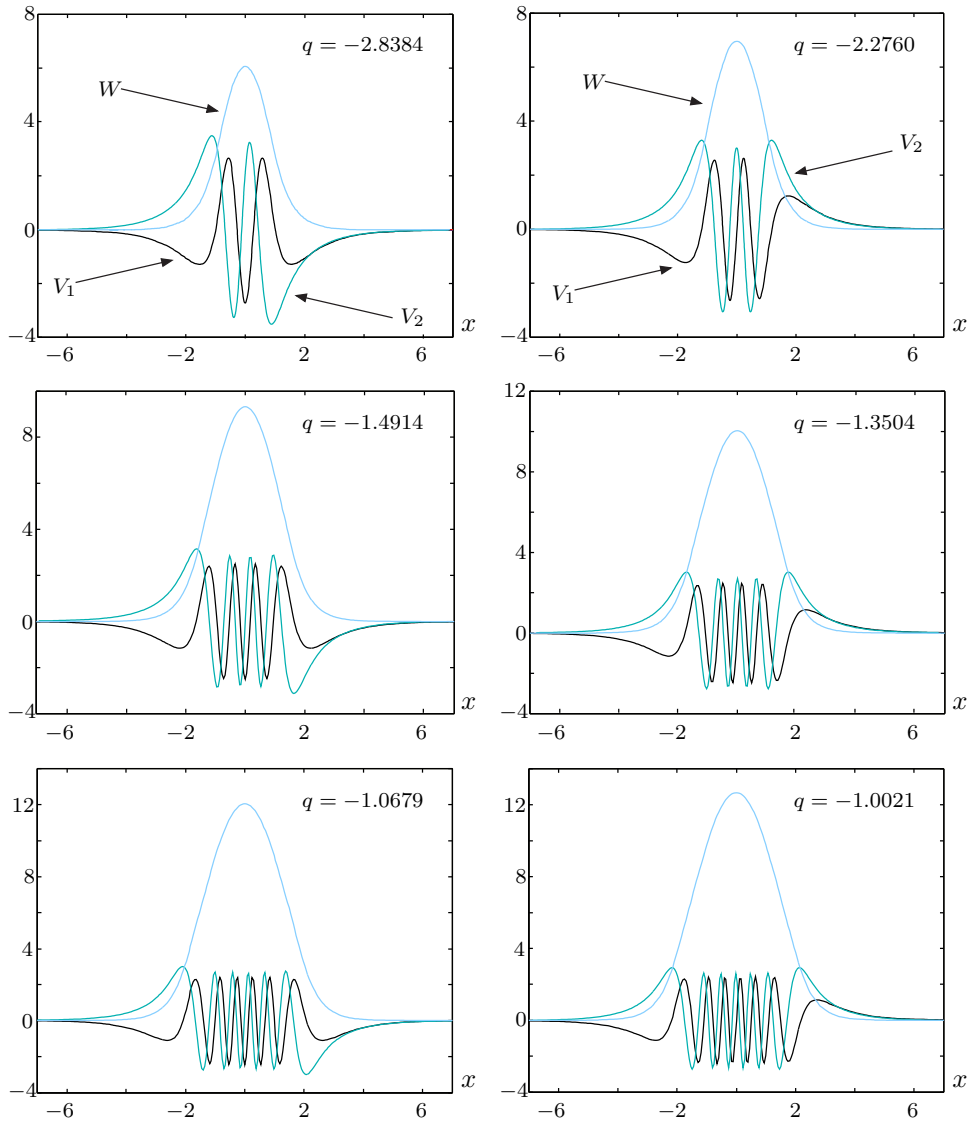

Figure 4